enzyme activities in serum and tissue lysates were measured as described (*25*).

28. Plasma samples were concentrated and buffer was exchanged with IEF sample buffer [7 M urea, 2 M thiourea, 50 mM tris (pH 7.5), 2% CHAPS, and 0.4% dithioerythritol] by diafiltration with 10-kD cutoff centrifugal filters (Millipore, Bedford, MA). Two-dimensional SDS-PAGE was carried out as described (*26*).
29. Two-dimensional blots were treated with 0.6% H_2O_2 in methanol for 30 min and blocked overnight at 4°C with 0.25% BSA (RIA grade, Sigma) in binding buffer (50 mM tris, 150 mM NaCl, and 4 mM $CaCl_2$, pH 7). Blots were incubated at room temperature with Con A–horseradish peroxidase (HRP) (EY Laboratories) at 1.8 μg/ml concentration in binding buffer, plus 10 mM α-methyl-glucopyranoside for 90 min. Blots were washed and then incubated with Chemiluminescence Reagent Plus (NEN Life Science) for 1 min before exposure on film.
30. We are grateful to E. Besmer, C. Nathan, J. Ravetch, and R. Steinman for discussions and suggestions; Y. Combarnous and O. Hindsgaul for pLH and S4GGnM- and GGnM-BSA, respectively; and Y. Hu and H. Nagaoka for assistance. This work was supported in part by Programme Grant G9601454 from the U.K. Medical Research Council (T. F), NIH Medical Scientist Training Program grant GM07739 (S.J.L.); and NIH and the Howard Hughes Medical Institute (M.C.N.).

4 January 2002; accepted 31 January 2002

Coordination of PIC Assembly and Chromatin Remodeling During Differentiation-Induced Gene Activation

Evi Soutoglou and Iannis Talianidis*

We analyzed the ordered recruitment of factors to the human α_1 antitrypsin promoter around the initial activation of the gene during enterocyte differentiation. We found that a complete preinitiation complex, including phosphorylated RNA pol II, was assembled at the promoter long before transcriptional activation. The histone acetyltransferases CBP and P/CAF were recruited subsequently, but local histone hyperacetylation was delayed. After transient recruitment of the human Brahma homolog hBrm, remodeling of the neighboring nucleosome coincided with transcription initiation. The results suggest that, at this promoter, chromatin reconfiguration is a defining step of the initiation process, acting after the assembly of the Pol II machinery.

Because packaging of DNA into chromatin causes a general repression of gene activity, reconfiguration of chromatin has been postulated to be mandatory for preinitiation complex (PIC) formation and transcriptional initiation (*1*–*3*). This is achieved by the adenosine triphosphate (ATP)–driven remodeling complexes, which act by altering nucleosome conformation, and by histone acetyltransferases (HATs), which covalently modify nucleosomal core histones (*4*–*6*). The current view suggests that these two types of proteins are first recruited by sequence-specific transcription factors to establish a local chromatin structure that is permissive for the subsequent assembly of an active PIC, including RNA pol II at the promoters (*1*, *2*). The in vivo sequence of nucleosome acetylation and remodeling events relative to transcriptional activation has been studied in two types of promoters. In the cell cycle–regulated yeast HO promoter, the Swi5p activator recruits the SWI/SNF remodeling complex, which then recruits the SAGA HAT complex. These two factors then facilitate the binding of a second activator (SBF) and the recruitment of the SRB/mediator complex, and these are followed by the Cdk1 activation-dependent association of RNA pol II with the promoter and transcription initiation (*7*–*9*). In the case of the virus-induced nucleosome-free interferon-β promoter, transient H4 hyperacetylation is required for remodeling of the neighboring nucleosome, which is essential for the general transcription factor TFIID recruitment and transcription initiation (*10*).

Because most active eukaryotic promoters are not nucleosome-free but are organized in precisely positioned nucleosomal arrays, we decided to study the relation between chromatin reconfiguration and PIC formation on the differentiation-induced α_1-antitrypsin ($\alpha_1$1-AT) gene. Our studies were conducted on CaCo-2 cells, which, upon reaching confluence, spontaneously differentiate from cryptlike to villuslike enterocytes and express several marker genes, including α_1-AT (*11*, *12*). Transcriptional activation of the α_1-AT gene requires the synergistic action of hepatocyte nuclear factors HNF-1α and HNF-4α (*13*, *14*).

The earliest time point when α_1-AT mRNA can be detected by reverse transcription–polymerase chain reaction (RT-PCR), nuclear run-on, or S-1 nuclease protection assays is at day 5.5 of the CaCo-2 cell-differentiation program (Fig. 1A). The ab-

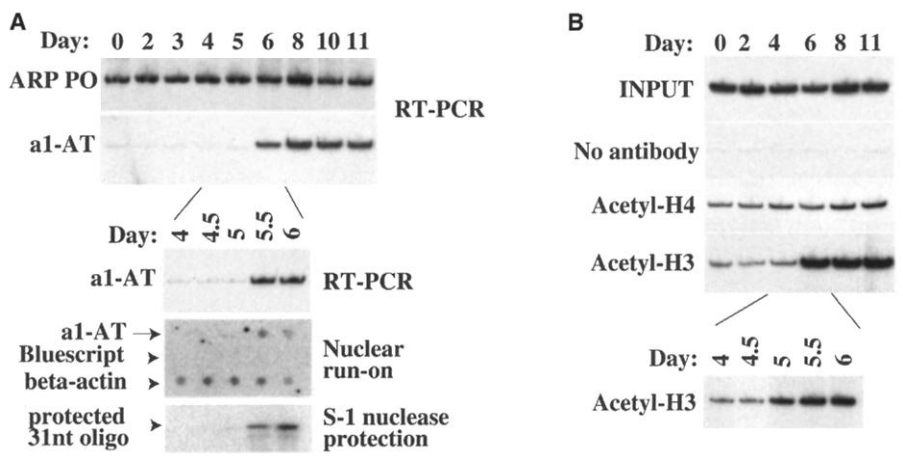

Fig. 1. Activation of the α_1-AT gene during enterocyte differentiation. (**A**) CaCo-2 cells were grown as described (*16*), and total RNA was prepared at the indicated days after the cells reached confluence (at day 0). Semiquantitative RT-PCR was performed with primers (*16*) spanning the α_1-AT or the acidic ribosomal phosphoprotein (ARP-PO) coding region. S-1 nuclease protection analysis with an antisense oligonucleotide corresponding to the +4 to +35 nt region of the α_1-AT gene and nuclear run-on assays with α_1-AT cDNA, bluescript vector, and beta-actin controls were performed essentially as in (*26*). (**B**) At the indicated time points, soluble chromatin from formaldehyde–cross linked CaCo-2 cells was prepared and immunoprecipitated with antibodies to acetyl-H3 or acetyl-H4 (Upstate Biotechnology), and the amounts of α_1-AT promoter–containing DNA in the immunoprecipitates were estimated by radioactive PCR (*16*). Aliquots (1/200) of total chromatin DNA before immunoprecipitation were processed similarly (INPUT).

Institute of Molecular Biology and Biotechnology, Foundation for Research and Technology Hellas, Post Office Box 1527, 711 10 Herakleion, Crete, Greece.

*To whom correspondence should be addressed. E-mail: talianid@imbb.forth.gr

sence of S-1 nuclease–protected oligonucleotide probe before day 5.5 indicates that no short 5′-truncated α_1-AT transcripts accumulate as a result of potential elongational pausing after nucleotide 35. The initial activation was preceded (at day 5) by selective histone H3 hyperacetylation at the proximal promoter region (Fig. 1B), confirming the role of nucleosome acetylation in transcription initiation (*15*). Low-resolution nucleosome mapping by indirect end labeling of micrococcal nuclease (MNase)–digested chromatin revealed that the α_1-AT promoter region was occupied by an array of positioned nucleosomes throughout the differentiation program (Fig. 2A). To map the exact borders of the nucleosomes positioned at the proximal promoter region, we performed ligation-mediated (LM)-PCR on formaldehyde–cross-linked mononucleosome preparations. Nucleosome 1 (NUC1) was found to be located between the –213 and –63 nucleotides (nt) relative to the transcription start site, and NUC2 was found between the –33 and +112 nt region (Fig. 2B). The binding sites for HNF-1α (–73 to –66 nt) and HNF-4α (–119 to –108 nt) were situated at the region covered by NUC1, and the TATA box (–25 to –19 nt) and the transcription start site were located at the region covered by NUC2 (Fig. 2D). No repositioning of NUC1 and NUC2 was evident during the differentiation process, regardless of transcription or the state of nucleosome acetylation of the α_1-AT gene (Fig. 2B). Restriction enzyme hypersensitivity assays in isolated nuclei, however, revealed changes in the conformation of NUC2. As expected, Bam HI hypersensitivity could be detected in all samples, because the restriction site was situated in the linker region (Fig. 2C). On the other hand, the Apa I site (–7 nt), located within NUC2 close to the transcription start site, was hypersensitive to the enzyme only in nuclei prepared from day-5.5 to day-8 postconfluent cells (Fig. 2C).

To investigate how these events correlate with PIC formation, we performed chromatin immunoprecipitation (Chip) experiments. HNF-1α, one of the major regulators of the α_1-AT gene, was found to be constitutively associated with the promoter (Fig. 3A). On the other hand, occupancy by the other regulator, HNF-4α, gradually increased from day 4, reaching a plateau at day 6 of differentiation. This pattern correlated with HNF-4α expression (*16*). Similar to HNF-1α, the general transcription factors TBP and TFIIB could be detected on the promoter on all days of the differentiation program (Fig. 3A). However, two other components of TFIID, TAFII-250 and TAFII-30, were absent from the promoter in predifferentiated cells (at day 0), suggesting that the TBP detected at this time point was not part of the classical TFIID complex (*17*, *18*). Recruitment of TAFs, TFIIH, components of the mediator complex (TRAP-220 and TRAP-100), and RNA pol II occurred at day 2 (Fig. 3A).

Because the TATA box of the α_1-AT promoter was located in a region organized in a nucleosome, we confirmed the binding of TBP to nucleosomal DNA in the same cells by performing the Chip assay with MNase-generated mononucleosome preparations. In this assay, primers spanning NUC2, but not primers from linker DNA, could efficiently amplify mononucleosomes precipitated by an antibody to TBP (Fig. 3, C and D). As expected, some signal, corresponding to immunoprecipitated NUC1, could also be observed, because cross-linking through intermediary factors could link NUC1 and NUC2 complexes. These data indicate that TBP either directly associated with NUC2 or that

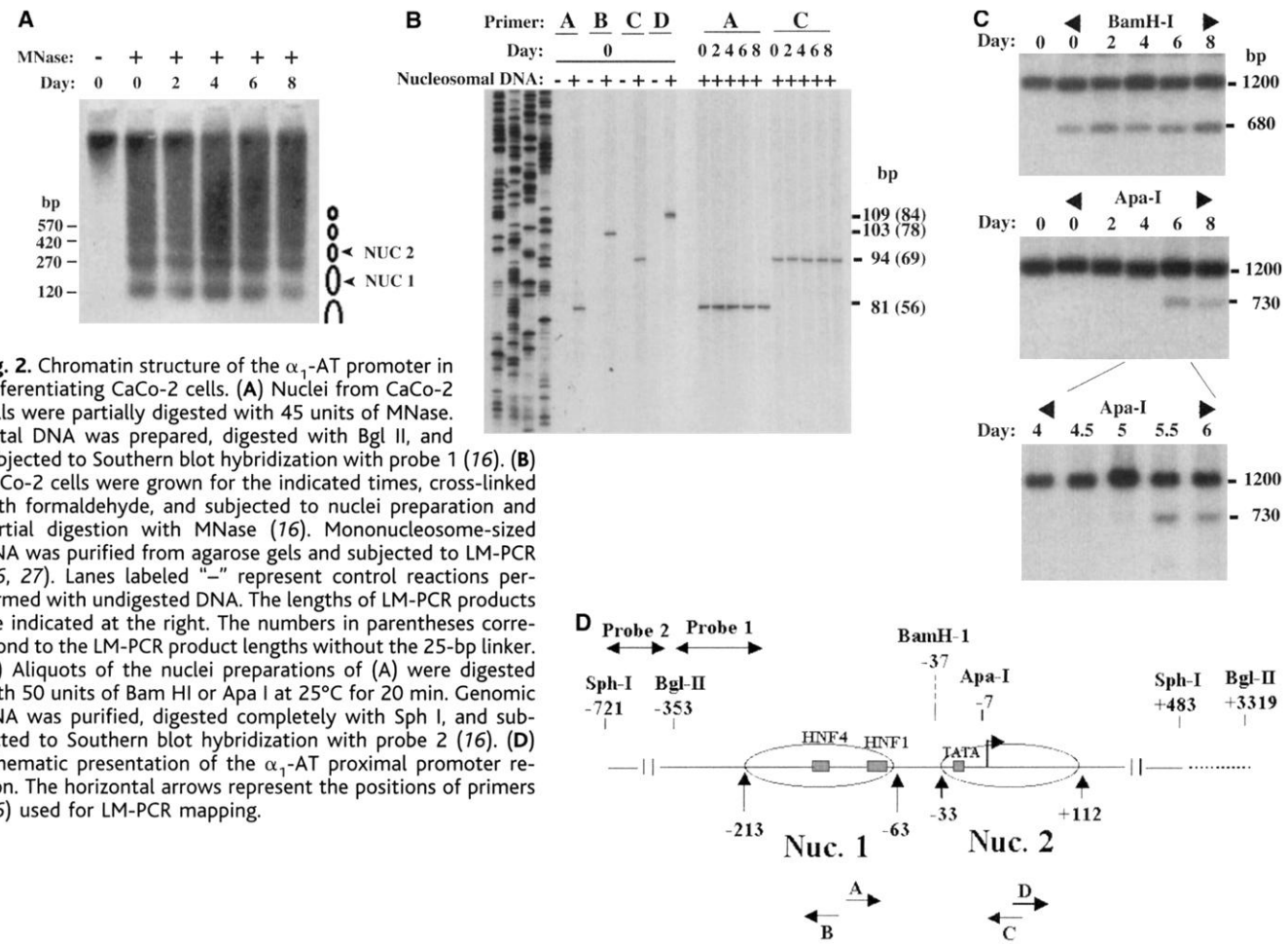

Fig. 2. Chromatin structure of the α_1-AT promoter in differentiating CaCo-2 cells. (**A**) Nuclei from CaCo-2 cells were partially digested with 45 units of MNase. Total DNA was prepared, digested with Bgl II, and subjected to Southern blot hybridization with probe 1 (*16*). (**B**) CaCo-2 cells were grown for the indicated times, cross-linked with formaldehyde, and subjected to nuclei preparation and partial digestion with MNase (*16*). Mononucleosome-sized DNA was purified from agarose gels and subjected to LM-PCR (*16*, *27*). Lanes labeled "–" represent control reactions performed with undigested DNA. The lengths of LM-PCR products are indicated at the right. The numbers in parentheses correspond to the LM-PCR product lengths without the 25-bp linker. (**C**) Aliquots of the nuclei preparations of (A) were digested with 50 units of Bam HI or Apa I at 25°C for 20 min. Genomic DNA was purified, digested completely with Sph I, and subjected to Southern blot hybridization with probe 2 (*16*). (**D**) Schematic presentation of the α_1-AT proximal promoter region. The horizontal arrows represent the positions of primers (*16*) used for LM-PCR mapping.

TBP may have protected its site from MNase cleavage. To confirm the first scenario, we performed re-Chip assays with TBP and H3 antibodies. NUC2-containing DNA could be detected in chromatin sequentially immunoprecipitated with TBP and H3 antibodies (Fig. 3E). This supports the notion that TBP associates with nucleosomal DNA.

Taken together, initially, HNF-1α, TFIIB, and TBP occupied the promoter, suggesting that chromatin was permissive for these protein-DNA interactions in vivo. This complex may represent a "poised" or "committed state" to mark the gene for subsequent events. The next step involved a potential exchange of a "TAF-less" TBP or a "nonclassical TFIID" complex (*17*, *18*) with a TAF-250 containing TFIID complex, which coincided with the recruitment of the other components of the PIC, including RNA pol II. Thus, all the major components of the general transcription factor machinery were stably assembled at the promoter several days before HAT recruitment, nucleosome acetylation, remodeling, and transcription initiation. This argues against the common view, supported mainly by in vitro reconstitution experiments, which suggests that chromatin reconfiguration is a prerequisite for PIC recruitment (*3*, *19*).

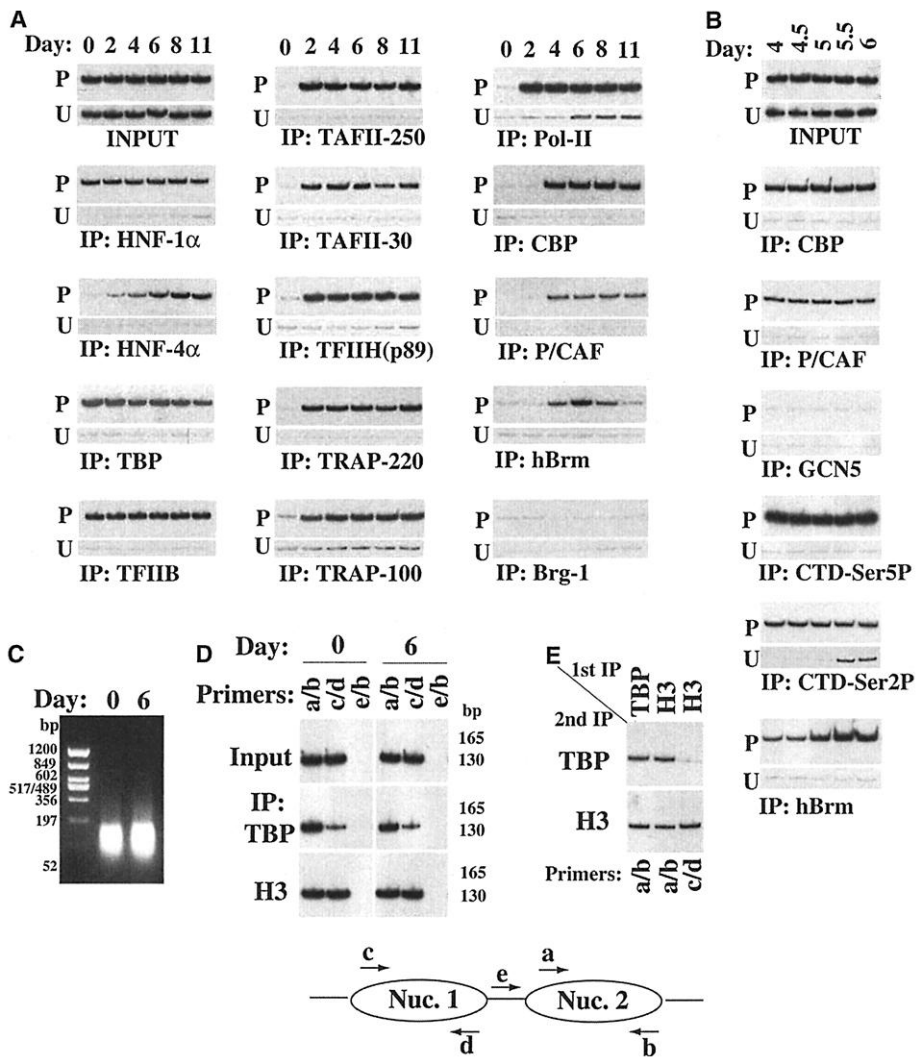

Fig. 3. Order of recruitment of PIC components on the α_1-AT promoter during CaCo-2 cell differentiation. (**A** and **B**) Chromatin immunoprecipitation experiments (*16*) were performed with antibodies against the indicated proteins (IP). PCR products corresponding to the α_1-AT proximal promoter (P) and α_1-AT 3′UTR region (U) were generated from an aliquot (1/200) of total chromatin (INPUT) or the immunoprecipitated materials. The numbers at the top indicate the time after the cells reached confluence. (**C** to **E**) After formaldehyde cross-linking, nuclei were prepared and digested with 850 μM units of MNase at 37°C for 30 min to obtain mononucleosome-sized fragments. An aliquot of the preparation was de–cross-linked, the purified DNA was analyzed by agarose gel electrophoresis (C), and the remaining part was subjected to Chip analysis with antibodies to TBP and H3 (D). Complexes immunoprecipitated with the indicated 1st antibodies were eluted from the Protein-G Sepharose beads and, after dilution, were reimmunoprecipitated with the indicated 2nd antibodies (*16*) (E). PCR reactions were performed with the primer sets indicated at the bottom.

Recruitment of CBP and P/CAF, which occurred after PIC assembly at day 4 (Fig. 3A), was accompanied by a delayed increase in nucleosome hyperacetylation. This suggests that either further interactions are required for full enzymatic activity (*20*) or that the accessibility of their nucleosomal substrates is suboptimal at this stage.

hBrm, but not Brg 1, associated transiently with the promoter from days 4 to 8 (Fig. 3, A and B). Its occupancy peaked at days 5.5 and 6, shortly after H3 hyperacetylation. This is consistent with the existence of a functional link between HAT and remodeling complexes (*21*, *22*). Although H3 hyperacetylation at the promoter persisted after transcription initiation, hBrm dissociated from it after remodeling NUC2. It seems therefore likely that acetylated histone tails, per se, are not sufficient for stable hBrm-nucleosome interactions and that the altered conformation adopted by the acetylated nucleosomes may in fact destabilize the complex. The release of hBrm from the promoter after the initial activation of the gene indicates that its activity was not required for subsequent rounds of reinitiation.

Because constant levels of all factors, except HNF-4α, were detected in extracts prepared at the different days (*16*), the sequential association of the complexes with the promoter could not be explained by changes in their expression during cell differentiation. The underlying mechanism would instead involve interdependent cooperative protein-protein interactions, by which different interaction surfaces of the individual components would be exposed at distinct steps of the assembly process. Although the pattern of HNF-4α recruitment correlated with the pattern of its expression levels, other mechanisms such as acetylation of HNF-4α may also contribute to its progressive association with the promoter. In line with this is the observation that acetylation of HNF-4α positively influenced its DNA binding activity (*23*).

The main events that took place at the time of initiation were the stable association of HNF-4α and hBrm with the promoter and remodeling of NUC2, which seems to be critical for Pol II release. Phosphorylation of the Pol II COOH-terminal domain (CTD) has been considered as a modification that controls the transition from initiation to elongation (*24*). We could detect some Pol II signal at the 3′-untranslated (3′-UTR) region of the gene at times of active transcription, because the Pol II antibody used can recognize both the initiating and elongating forms of the polymerase (*16*). When antibodies against the phosphorylated (CTD) of RNA pol II were used, we found that both Ser-5– and Ser-2–phosphorylated forms of Pol II were associated with the promoter (Fig. 3B). Ser-2– but

not Ser-5–phosphorylated Pol II could be detected at the downstream region after day 5.5, which is consistent in part with the recent finding that Pol II-S5P is localized to promoters, whereas Pol II-S2P can be observed in coding regions (*25*). The finding that both Ser-5– and Ser-2–phosphorylated forms of Pol II were present at the α_1-AT promoter from the day of recruitment and long before transcription could be detected suggests that CTD phosphorylation is not sufficient for Pol II release. This could occur only when NUC-2 became remodeled, pointing to a previously unknown regulatory function of nucleosome structure. When situated around the transcription start site, the nucleosome may act as a barrier that controls the escape of RNA pol II from the promoter. In the case of the α_1-AT gene, nucleosome reconfiguration is the final determining step of the initiation process.

References and Notes

1. B. Lemon, R. Tjian, *Genes Dev.* **14**, 2551 (2000).
2. K. Struhl, *Cell* **98**, 1 (1999).
3. C. J. Fry, C. L. Peterson, *Curr. Biol.* **11**, R185 (2001).
4. C. L. Peterson, J. L. Workman, *Curr. Opin. Genet. Dev.* **10**, 187 (2000).
5. R. E. Kingston, G. J. Narlikar, *Genes Dev.* **13**, 2339 (1999).
6. B. D. Strahl, C. D. Allis, *Nature* **403**, 41 (2000).
7. M. P. Cosma, T. Tanaka, K. Nasmyth, *Cell* **97**, 299 (1999).
8. M. P. Cosma, S. Panizza, K. Nasmyth, *Mol. Cell* **7**, 1213 (2001).
9. L. T. Bhoite, Y. Yu, D. J. Stillman, *Genes Dev.* **15**, 2457 (2001).
10. T. Agalioti *et al.*, *Cell* **103**, 667 (2000).
11. M. D. Peterson, M. S. Mooseker, *J. Cell Sci.* **102**, 581 (1992).
12. D. H. Perlmutter *et al.*, *J. Biol. Chem.* **264**, 9485 (1989).
13. P. Monaci, A. Nicosia, R. Cortese, *EMBO J.* **7**, 2075 (1988).
14. C. Hu, D. H. Perlmutter, *Am. J. Physiol.* **276**, G1181 (1999).
15. K. Struhl, *Genes Dev.* **12**, 599 (1998).
16. Supplementary information can be found on *Science* Online at www.sciencemag.org/cgi/content/full/295/5561/1901/DC1.
17. B. Bell, L. Tora, *Exp. Cell Res.* **246**, 11 (1999).
18. S. R. Albright, R. Tjian, *Gene* **242**, 1 (2000).
19. F. J. Dilworth, C. Fromental-Ramain, K. Yamamoto, P. Chambon, *Mol. Cell* **6**, 1049 (2000).
20. E. Soutoglou *et al.*, *EMBO J.* **20**, 1984 (2001).
21. A. H. Hassan, K. E. Neely, J. L. Workman, *Cell* **104**, 817 (2001).
22. P. Syntichaki, I. Topalidou, G. Thireos, *Nature* **404**, 414 (2000).
23. E. Soutoglou, N. Katrakili, I. Talianidis, *Mol. Cell* **5**, 745 (2000).
24. M. E. Dahmus, *J. Biol. Chem.* **271**, 19009 (1996).
25. P. Komarnitsky, E.-J. Cho, S. Buratowsky, *Genes Dev.* **14**, 2452 (2000).
26. M. E. Greenberg, in *Current Protocols in Molecular Biology*, M. Ausubel *et al.*, Eds. (Wiley, New York, 1999) vol. 1, chap. 4.
27. C. E. McPherson, E. Y. Shim, D. S. Friedman, K. S. Zaret, *Cell* **75**, 387 (1993).

28. Supported by grants from the Greek General Secretariat for Science and Technology (PENED-99ED-636), European Union (HPRN-CT-2000-00087), and Human Frontier Science Program (RGP-0024). We thank L. Tora and Y. Nakatani for antibody reagents, N. Katrakili for expert technical assistance, and P. Hatzis and G. Thireos for helpful discussions and comments on the manuscript.

26 November 2001; accepted 18 January 2002

Purkinje cell degeneration (*pcd*) Phenotypes Caused by Mutations in the Axotomy-Induced Gene, *Nna1*

Angeles Fernandez-Gonzalez,[1]* Albert R. La Spada,[2]* Jason Treadaway,[1] Jason C. Higdon,[1] Belinda S. Harris,[3] Richard L. Sidman,[4] James I. Morgan,[1] Jian Zuo[1]†

The classical recessive mouse mutant, *Purkinje cell degeneration* (*pcd*), exhibits adult-onset degeneration of cerebellar Purkinje neurons, retinal photoreceptors, olfactory bulb mitral neurons, and selected thalamic neurons, and has defective spermatogenesis. Here we identify *Nna1* as the gene mutated in the original *pcd* and two additional *pcd* alleles (pcd^{2J} and pcd^{3J}). *Nna1* encodes a putative nuclear protein containing a zinc carboxypeptidase domain initially identified by its induction in spinal motor neurons during axonal regeneration. The present study suggests an unexpected molecular link between neuronal degeneration and regeneration, and its results have potential implications for neurodegenerative diseases and male infertility.

Strains of mice harboring mutations that affect the nervous system have provided important insights into normal and aberrant neural development and function (*1–3*). Although the genes responsible for many of the classical neurological mutants have been identified, the *Purkinje cell degeneration* (*pcd*) gene remains elusive. Unlike many mouse mutants in which neuronal loss occurs during development (*2*, *3*), *pcd* is unusual in that neurodegeneration occurs after weaning, when most synaptic circuitries are established. Thus, the identification of the gene responsible for the *pcd* phenotype could provide a key molecular entry point into pathways or processes underlying other neurodegenerative disorders in humans.

The original *pcd* mutation (referred to here as "pcd^{1J}", to distinguish it from later-occurring *pcd* mutations) arose spontaneously in the C57BR/cdJ strain and exhibits ataxia resulting from loss of cerebellar Purkinje cells during early adulthood (*4*, *5*). Populations of thalamic neurons also degenerate between postnatal days 50 and 60 in pcd^{1J} (*6*, *7*), whereas degeneration of retinal photoreceptors and olfactory bulb mitral cells progresses slowly over a year (*8–11*). Also, adult male pcd^{1J} mice are infertile because they have reduced numbers of sperm that are abnormally shaped and nonmotile (*5*, *12*). Two additional *pcd* alleles, pcd^{2J} and pcd^{3J}, arose spontaneously in SM/J and BALB/cByJ mouse strains, respectively. The pcd^{2J} allele was maintained in C57BL/6J congenic lines for >15 backcross generations. The phenotypes of pcd^{1J} and pcd^{3J} homozygotes were nearly iden-

[1]Department of Developmental Neurobiology, St. Jude Children's Research Hospital, Memphis, TN 38105, USA. [2]Department of Laboratory Medicine and Division of Medical Genetics (Medicine), University of Washington, Seattle, WA 98195–7110, USA. [3]The Jackson Laboratory, Bar Harbor, ME 04609, USA. [4]Harvard Medical School and Department of Neurology, Beth Israel Deaconess Medical Center, Boston, MA 02115, USA.

*These authors contributed equally to this work.
†To whom correspondence should be addressed. E-mail: jian.zuo@stjude.org

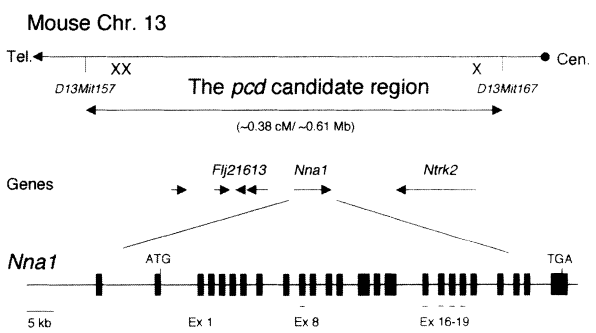

Fig. 1. Genetic mapping of *pcd* and gene structure of *Nna1*. The *pcd* locus was mapped to mouse chromosome 13 between *D13Mit167* and *D13Mit157*. Three crossovers (two telomeric, "XX" and one centromeric, "X") defined the boundaries of the *pcd* candidate region. The *pcd* cosyntenic region of human (9q21.33–9q22.1) contains six predicted genes (indicated by lines and their 3′ ends indicated by arrows); *Ntrk2* and *Flj21613* flank *Nna1*. Filled squares, exons; ATG, initiation codon; TGA, stop codon. Exons 8 and 16 to 19 (underlined) were used as probes for Northern and in situ hybridization analyses.